Published in final edited form as:
Mol Imaging. 2014 April 1; 16(0): 1–9.

Ultrasound Detection of Myocardial Ischemic Memory Using an E-Selectin Targeting Peptide Amenable to Human Application

Xiaoping Leng[#], **Jianjun Wang**[#], **Andrew Carson**, **Xucai Chen**, **Huili Fu**, **Susanne Ottoboni**, **William R. Wagner**, and **Flordeliza S. Villanueva**

Department of Ultrasound, the Second Affiliated Hospital of Harbin Medical University, the Key Laboratory of Myocardial Ischemia, Chinese Ministry of Education, Harbin, China; Center for Ultrasound Molecular Imaging and Therapeutics and McGowan Institute for Regenerative Medicine, University of Pittsburgh, Pittsburgh, PA; and Depomed, Inc., Newark, CA.

[#] These authors contributed equally to this work.

Abstract

Vascular endothelial leukocyte adhesion molecules, such as E-selectin, are acutely upregulated in myocardial ischemia/reperfusion and are thus “ischemic memory” biomarkers for recent cardiac ischemia. We sought to develop an ultrasound molecular imaging agent composed of microbubbles (MBs) targeted to E-selectin to enable the differential diagnosis of myocardial ischemia in patients presenting with chest pain of unclear etiology. Biodegradable polymer MBs were prepared bearing a peptide with specific human E-selectin affinity (MB_{ESEL}). Control MBs had scrambled peptide (MB_{CTL}) or nonspecific IgG (MB_{IgG}). MB_{ESEL} adhesion to activated rat endothelial cells (ECs) was confirmed in vitro in a flow system and in vivo with intravital microscopy of rat cremaster microcirculation. Ultrasound molecular imaging of recent myocardial ischemia was performed in rats 4 hours after transient (15 minutes) coronary occlusion. MB_{ESEL} adhesion was higher to inflamed versus normal ECs in vitro; there was no difference in MB_{CTL} or MB_{IgG} adhesion to inflamed versus normal ECs. There was greater adhesion of MB_{ESEL} to inflamed versus noninflamed microcirculation and minimal adhesion of MB_{CTL} or MB_{IgG} under any condition. Ultrasound imaging after injection of MB_{SEL} demonstrated persistent contrast enhancement of the previously ischemic region. Videointensity in postischemic myocardium after MB_{ESEL} was higher than that in the nonischemic bed (11.6 ± 2.7 dB vs 3.6 ± 0.8 dB, $p < .02$) and higher than that after MB_{CTL} (4.0 ± 1.0 dB, $p < .03$) or MB_{IgG} (1.7 ± 0.1 dB, $p < .03$). MBs targeted to E-selectin via a short synthetic peptide with human E-selectin binding affinity enables echocardiographic detection of recent ischemia, setting the stage for clinical myocardial ischemic memory imaging to identify acute coronary syndromes.

The diagnosis of acute coronary syndrome (ACS) in patients presenting to the emergency department with a history of recent or ongoing chest pain can be a challenge, particularly in

Address reprint requests to: Flordeliza S. Villanueva, MD, Center for Ultrasound Molecular Imaging and Therapeutics, Heart and Vascular Institute, University of Pittsburgh, A351 Presbyterian University Hospital, 200 Lothrop Street, Pittsburgh, PA 15213; villanuevafs@upmc.edu..

Financial disclosure of reviewers: None reported.

patients presenting with atypical symptoms and signs. True acute myocardial ischemia is associated with upregulation of leukocyte adhesion molecules, such as P-selectin, E-selectin, and intracellular adhesion molecule 1 (ICAM-1), which hence provide a molecular signature, or tissue memory, of a recent ischemic event.[1] Ultrasound molecular imaging (UMI)[2] to identify overexpression of leukocyte adhesion molecules may offer an approach to the detection of recent myocardial ischemia. This technique relies on ultrasound detection of disease-specific endothelial epitopes using gas-filled microbubbles (MBs) as probes that bind specifically to the epitopes via targeting moieties on the surface of MBs.

We previously proved the concept of echocardio-graphic ischemic memory imaging using MBs targeted to P-selectin via the naturally occurring tetrasaccharide ligand sialyl Lewis X (sLeX).[3] Because such MBs are not ideal for clinical use due to the complex carbohydrate chemistry[4] and possible immunogenicity,[5,6] we sought to develop an ischemic memory UMI probe that could be more readily extended to humans. We hypothesized that UMI for ischemic memory could be achieved using a double-layer MB contrast agent previously used safely in humans,[7,8] now conjugated to an E-selectin-specific 12-mer synthetic peptide on the surface.

Methods

MB Preparation

The contrast agent was a double-layer MB composed of an outer shell of crosslinked human albumin, an inner layer of biodegradable polymer (poly-DL-lactide [PDLLA]), and encapsulated nitrogen gas.[9] The surface of the MBs was coated with biotin for further targeting ligand attachment.[10] For intravital microscopy, the MBs were fluorescently labeled with Bodipy 493/503 (Life Technologies, Eugene, OR). Biotinylated peptide AF10166 (H2N-DITWDQLWDLMK-COOH, Peptides International), previously identified by phage display to have specific affinity to human E-selectin, was used as the targeting moiety.[11] The control ligands were either a biotinylated peptide composed of a random AF10166 sequence 12-mer (H_2N-WKLDTLDMIWQD-COOH) or rat biotinylated immunoglobulin G (IgG, BD Biosciences, San Diego, CA). The ligands were conjugated onto the MB via biotinstreptavidin bridging chemistry. MBs conjugated with AF10166 are henceforth designated as MB_{ESEL}, and MBs linked to the 12-mer randomized sequence or IgG are designated as MB_{CTL} and MB_{IgG}, respectively. MB diameter was 3.4 ± 1.3 μm (Multisizer-III, Beckman Coulter, Beckman Coulter, Miami, FL).

In Vitro Parallel Plate Perfusion

A parallel plate perfusion chamber was used to quantify MB adhesion to cultured endothelial cells (ECs).[12] Rat heart microvascular ECs (VEC Technologies, Rensselaer, NY) were grown to confluence on 25 mm × 75 mm glass coverslips. Cells were incubated for 5 hours with 5 ng/mL interleukin-1β (Sigma-Aldrich, St. Louis, MO) to cause activation. Coverslips with normal or IL-1β-activated ECs (n = 3/condition) were mounted in the chamber and perfused with one of the three MB species (5×10^6 MB in 1 mL culture medium) at a wall shear rate of 200 s^{-1}, followed by an additional 3 mL of plain culture medium. The chamber was then mounted on a microscope (Nikon TE200) and 20 random

bright-field images (× 100) of the ECs were captured (ORCA285, Hamamatsu, Bridgewater, NJ). The mean number of attached MBs/ECs was counted offline.

In Vivo Studies

All protocols were approved by the Institutional Animal Care and Use Committee at the University of Pittsburgh. Wistar rats (Sprague Dawley, Harlan Laboratories, Indianapolis, IN) were anesthetized with intraperitoneal sodium pentobarbital (50 mg/kg) and maintained with 1.5 to 2.0% inhaled isoflurane. Body temperature was maintained at 37°C with a heating pad. The internal jugular vein was canulated with a 20-gauge catheter for MB injection.

Intravital Microscopy

Microscopy of the rat cremaster muscle microcirculation was used for real-time visualization of MB adhesion in vivo. Sprague Dawley rats (100–120 g) received intrascrotal injection of either tumor necrosis factor α (*n* = 9, 5 μg, Thermo Scientific, Waltham, MA) or 1 mL saline (*n* = 9). Four hours later, the cremaster muscle was exteriorized and mounted on an inverted fluorescent microscope (Nikon TE200). Each rat received one intravenous injection (1×10^8 MB) of either MB_{ESEL} or control MBs (MB_{CTL} or MB_{IgG}) in 200 μL saline, followed by a 200 μL saline flush (*n* = 3 rats per MB type/inflammatory status combination, total 6 groups). Five minutes after injection, bright-field microscopic imaging of 20 random fields was performed to identify microvessels, and epi-illumination fluorescent imaging was performed to identify MBs, followed by pentobarbital overdose. Images were analyzed offline for MB adhesion per field of view, defined as MB immobility lasting ≥ 30 seconds.

UMI of Myocardium

A previously described rat model of acute myocardial ischemia and reperfusion[3] was used for UMI of E-selectin overexpression as a marker of ischemic memory. Anesthetized rats (*n* = 6, 150–200 g) were intubated and mechanically ventilated. A lateral thoracotomy was performed, and the left anterior descending (LAD) coronary artery was occluded for 15 minutes and then reperfused. After 4 hours of reflow, each rat received separate intravenous injections of MB_{ESEL}, MB_{CTL}, and MB_{IgG} in random order (2.5×10^7 MBs in 200 μL saline followed by a 200 mL saline flush), and ultrasound imaging was performed as described below. Thereafter, high mechanical index (MI) burst pulses were sent to ensure that all adhered and freely circulating MBs were destroyed prior to any subsequent injection. Typically, subsequent injections were given 5 minutes after MBs could no longer be detected in the left ventricular cavity on ultrasound imaging. The MB dosage was empirically chosen based on pilot studies assessing myocardial enhancement from various doses. At the end of the experiment, the LAD coronary artery was reoccluded, nontargeted myocardial contrast echocardiography (MCE) using plain lipid MBs was performed to delineate the risk area, and the rat was euthanized using pentobarbital overdose.

Open-chest MCE in the short-axis view was performed using a contrast-specific imaging mode combining phase and amplitude modulation of the transmit signal (Cadence Contrast Pulse Sequencing, Sequoia 512, Siemens Ultrasound, Mountain View, CA) from a linear

array transducer (15L8) operating at 8 MHz. Probe position, dynamic range, gain settings, and focus were initially optimized and maintained constant. Ultrasound detection of bound MBs was performed using a previously described approach.[12,13] After 3 minutes to allow MB retention and washout of unbound MBs, end-systolic imaging was performed at an MI of 0.6, followed by an ultrasound burst pulse at MI of 1.9 to destroy the MBs and then end-systolic imaging 30 seconds later at MI 0.6. The imaging time at 3 minutes post-MB injection was determined from pilot contrast imaging studies demonstrating that by 3 minutes after injection, background signal from freely circulating MBs is minimal. The postdestruction frames were subtracted from the predestruction frames to form a single color-coded image to represent the signal attributable to MB adhesion as previously described.[14] Mean videointensity (VI) was measured in the ischemic and nonischemic beds. Using a two-way random effects model, interobserver agreement in VI measurement by three independent examiners was high (intraclass correlation coefficient of 0.99 and 0.97 for ischemic and nonischemic beds, respectively).

Quantification of Myocardial Inflammation and Infarction

Postmortem, the heart was excised and sectioned into three short-axis slices for 2,3,5-triphenyl tetrazolium chloride (TTC) staining to delineate infarction.[15] Other myocardial pieces were snap-frozen in liquid nitrogen for immunohistochemistry and real-time polymerase chain reaction (RT-PCR) to quantify E-selectin expression.

Immunohistochemical staining of myocardial sections was performed to detect E-selectin and ICAM-1. Cryostat sections (5 mm) were fixed in ice-cold acetone and air dried. After blocking nonspecific protein binding with 2% bovine serum albumin in phosphate-buffered saline, sections were incubated overnight with goat polyclonal antirat E-selectin antibody (15 μg/mL, R&D Systems, Minneapolis, MN) or goat polyclonal antirat ICAM-1 antibody at 4°C, followed by incubation with Cy3-conjugated donkey anti-goat secondary antibody (diluted 1:2,000) or fluorescein isothiocyanate (FITC)-conjugated donkey antigoat secondary antibody (Santa Cruz Biotechnology, Dallas, TX) for 2 hours at room temperature. For negative controls, specific antibodies were replaced by nonspecific rat IgG of the same isotype. Sections were counterstained with 4’,6-diamidino-2-phenylindole (Sigma-Aldrich), mounted, and examined microscopically.

RT-PCR was performed to quantify myocardial messenger ribonucleic acid (mRNA) expression of E-selectin and ICAM-1. Briefly, ribonucleic acid was extracted from tissue samples using Trizol reagent (Invitrogen, Carlsbad, CA), and complementary DNA was prepared using Taqman reverse transcriptase reagents (Applied Biosystems, Foster City, CA). Primers for E-selectin and ICAM-1, respectively, were 5’-GATGAAGCAAGTGCGTAT-3’ and 3’-GATGTAGGTTTCTGGGTT-5’, and 5’-AAACGGGAGATGAA2TGGT-3’ and 3’-ATGTGGATAATGGCGGTCT-5’. The glyceraldehyde-3-phosphate dehydrogenase (GAPDH) gene (primers 5’-GGCAAATTCAACGGCACAGT-3’ and 3’-CCCTTCGGGTAGTGGTAGA-5’) was used as a reference to normalize E-selectin and ICAM-1 measurements. RTPCR amplifications were conducted with the Absolute Blue SYBR Green/ROX kit (Thermo Scientific, Waltham, MA) on an ABI Prism 7000 sequence detection system (Applied Biosystems). E-

selectin and ICAM-1 expression were calculated by the ΔΔCt method and normalized to GAPDH expression in the same sample. The calculated values were expressed as fold increase over nonischemic myocardium.

Statistical Analysis

The results are expressed as mean ± SD. Data were compared with two-tailed Student *t*-tests. Statistical significance was defined as $p < .05$. The relationship between the size of the risk area and the size of the region of postischemic contrast enhancement was assessed using linear regression analysis.

Results

In Vitro Parallel Plate Perfusion Study

There was greater MB_{ESEL} adhesion to inflamed compared to noninflamed cells (17.4 ± 1.8 vs 5.9 ± 3.4 MB/EC, $p < .02$) (Figure 1). There was greater adhesion of MB_{ESEL} to inflamed ECs (17.4 ± 1.8 MB/EC) compared to MB_{CTL} (4.1 ± 0.6 MB/EC, $p < .02$) and MB_{IgG} (2.3 ± 0.6 MB/EC, $p < .01$). There was no difference in adhesion to activated versus normal ECs for MB_{CTL} ($p = .41$) or MB_{IgG} ($p = .48$).

Intravital Microscopy

There was greater adhesion of MB_{ESEL} to inflamed microcirculation (4.8 ± 1.2 MBs/field) compared to control MB_{IgG} (1.1 ± 0.3 MBs/field, $p < .03$) and MB_{CTL} (1.5 ± 0.3 MBs/field, $p < .04$) and compared to control, noninflamed microcirculation (1.7 ± 0.4 MBs/field; $p < .04$) (Figure 2). Figure 3 illustrates fluorescence images of venular segments under basal (panels D to F) and TNF-α-activated (panels A to C) conditions. There was attachment of Bodipy-labeled MB_{ESEL} under inflammatory conditions (Figure 3A), which was less frequently seen under basal conditions (Figure 3D). There was minimal attachment of MB_{CTL} (Figure 3, B and E) or MB_{IgG} (Figure 3, C and F) to normal or inflamed venules.

E-Selectin Targeted UMI

Figure 4 illustrates background-subtracted color-coded contrast ultrasound images from a single rat during occlusion and reperfusion. During LAD coronary artery occlusion, injection of nontargeted MBs confirmed the presence of a risk area involving the anterior septum and anterior wall (see arrows, Figure 4A). After release of the occlusion, nontargeted MCE showed resolution of the risk area (see Figure 4B). Figure 4D is a color-coded image 3 minutes after injection of MB_{ESEL}, after subtraction of the postdestruction frame. There was persistent contrast enhancement within a region that colocalized with the previously ischemic area LAD coronary artery territory, consistent with MB_{ESEL} binding to the postischemic bed. There was minimal persistent contrast enhancement after injection of either of the control MB species (Figure 4, E and F). TTC staining confirmed the absence of infarction (see Figure 4C).

Background-subtracted VI data in the ischemic and nonischemic myocardium 3 minutes after MB injection are shown in Figure 5. There was greater enhancement of the postischemic bed compared to the nonischemic bed after injection of the MB_{ESEL} (11.6 ±

2.7 dB vs 3.6 ± 0.8 dB; $p < .02$). Furthermore, contrast enhancement of the LAD coronary artery bed was higher after injection of MB_{ESEL} compared to the control MB_{CTL} (4.0 ± 1.0 dB; $p < .03$) and MB_{IgG} (1.7 ± 0.1 dB; $p < .03$). A significant linear relationship was found between the size of the risk area during coronary occlusion and the size of the region of persistent contrast enhancement after MB_{ESEL} injection ($y = 0.98\times - 0.01$, $r = .92$, risk area size data not shown).

Confirmation of Leukocyte Adhesion Molecule Upregulation

Immunofluorescent staining in all rats consistently confirmed microvascular E-selectin and ICAM-1 expression in postischemic myocardium that was minimally seen in the nonischemic bed. Examples from one rat are shown in Figure 6. Quantitative RT-PCR in all six rats indicated a 3.3-fold ($p < .03$) and 3.2-fold ($p < .02$) upregulation of E-selectin and ICAM-1 mRNA, respectively, in the ischemic bed relative to the nonischemic bed of the same heart.

Discussion

The main finding of this study is that postischemic myocardium can be identified with ultrasound imaging using E-selectin-targeted MBs. Importantly, the MBs were targeted via a short peptide having specific affinity to human E-selectin, which has distinct clinical advantages over previously used antibody[16,17] or carbohydrate-targeting strategies,[3,18] which confer immunogenicity or require complex synthetic chemistry, respectively. Thus, these data set the stage for human trials of bedside ischemic memory imaging in patients presenting with chest pain of possible ischemic etiology.

Challenges in Diagnosing ACS

Chest pain of possible cardiac origin accounts for 5 to 6 million emergency department visits annually.[19] Due to the resolution of symptoms by the time of presentation, atypical symptoms, and/or a nondiagnostic electrocardiogram, the diagnosis of true ACS can be elusive. Patients with true myocardial ischemia who are inappropriately discharged from the emergency department suffer high mortality and morbidity.[20,21] To avoid missing the diagnosis of ACS, physicians conservatively admit two to three patients for every one with true ACS, resulting in a large economic burden. Despite a conservative admission strategy, the diagnosis of true ACS is still missed in 2 to 7% of patients, underscoring the limitations in current tools for accurately identifying ACS. A rapid and noninvasive method for detecting true ongoing or recent myocardial ischemia would have both a high economic and a clinical impact. However, current methods such as electrocardiography,[22] troponin detection,[23] stress radionuclide single-photon emission computed tomography (SPECT),[24] and cardiac computed tomographic (CT) angiography[25] have limitations in diagnosing ACS. In particular, the most commonly employed imaging method for triaging patients presenting with chest pain, stress perfusion testing, detects impairment in flow reserve, which occurs in, and therefore does not distinguish among, stable coronary stenotic lesions,[26] recent myocardial ischemia from an unstable plaque,[27] or previous infarction.[28]

Molecular Imaging for Detecting Myocardial Ischemia

A molecular imaging approach to detect acute myocardial ischemia has inherent advantages over anatomic (cardiac CT) or physiologic (stress testing) imaging methods. An imaging probe targeted to a molecular or metabolic consequence of ischemia potentially offers higher specificity in detecting ACS as a cause of chest pain. For example, Dilsizian and colleagues used a radioactive fatty acid tracer, β-methyl-*p*-[^{123}I]-iodophenyl-pentadecanoic acid (BMIPP), to detect ischemia-induced shift to glucose metabolism as a marker of ischemic memory.[29] In patients with thallium^{201} treadmill exercise–induced ischemia, BMIPP injection and SPECT up to 22 hours after the ischemia showed reduced BMIPP uptake in myocardial segments with reduced ^{201}thallium uptake. Although promising, this method entails patient exposure to radioactivity and specialized cameras and is still in investigational stages.

Our approach used MBs as an acoustic imaging probe to bind endothelial leukocyte adhesion molecules that are upregulated after myocardial ischemia and reperfusion. We chose E-selectin, which mediates initial weak attachment of activated leukocytes to ECs and neutrophil recruitment to the myocardium.[30] E-selectin requires de novo synthesis and is transcriptionally regulated, appearing on endothelium within hours of ischemia and reperfusion, reaching a maximum at 2 to 4 hours after stimulation, and decreasing by 24 hours thereafter.[31,32] Cell surface expression of E-selectin protein parallels that of the mRNA. In our current study, immunofluorescent staining and RT-PCR showed E-selectin upregulation only in postischemic myocardium, making E-selectin a strong candidate for molecular imaging of ischemic memory. Furthermore, the time course of E-selectin expression—lasting hours after ischemic insult—offers a clinically practical time window for useful imaging, potentially allowing for diagnostic molecular imaging of ischemic memory for the significant number of patients who do not present to the emergency department immediately after the onset of chest pain.

Advantages of Polymer MB/Peptide Construct for Clinical Translation

Ultrasound studies targeting leukocyte adhesion molecules have been previously reported. MBs bearing monoclonal antibodies targeted to P-selectin ultrasonically detected recent myocardial ischemia in mice.[16] We have previously targeted P-selectin via the native ligand sLeX to identify recent ischemia.[3] Unlike the present study, however, these earlier studies used MB formulations that are not optimally suited for human translation due to the immunogenicity of antibodies or complex carbohydrate chemistry involved in the synthesis and MB conjugation of sLeX. Davidson and colleagues recently reported ischemic memory imaging using selectin-targeted MBs bearing a P-selectin glycoprotein ligand, which may have promise for human translation, but synthesis of the ligand involves complex recombinant methods and purification and is costly.[33]

Our study is the first to use a polymer MB conjugated to a peptide for molecular imaging. This construct potentially overcomes some of the current hurdles to clinical translation of previously described ultrasound contrast agents for molecular imaging. The dual-layer MB shell results in high stability, high echogenicity, and low immunogenicity.[10] The short

peptide ligand offers simple chemistry, should not have the immunogenicity of monoclonal antibodies, and, unlike other ligands reported for UMI of ischemic memory, is inexpensive.

AF10166 is a 12-mer peptide with high affinity (IC_{50} = 4.4 nM) to human E-selectin. Binding of AF10166 to human E-selectin blocks neutrophil adhesion in both static and flow-cell assays.[11] When the AF10166 peptide was attached to the MB shell, the targeted MBs bound to inflamed cultured ECs under flow conditions. Postischemic myocardium was persistently echogenic after targeted MB injection, consistent with microvascular adhesion of the targeted MBs. Given that the peptide was identified using phage display against human cells, binding to human E-selectin in vivo might be even more robust, resulting in images superior to those obtained in the current rat study.

It should be noted that other myocardial inflammatory conditions associated with E-selectin overexpression, such as acute myocarditis or heart transplant rejection,[14] would also be detected by our imaging method. However, these conditions would show a spatial pattern of diffuse, persistent contrast enhancement,[14] whereas recent acute ischemia from epicardial coronary obstruction results in contrast persistence in a vascular territory distribution (see Figure 4D).

Study Limitations

Our in vivo study modeled a transient total coronary occlusion and ischemic memory 4 hours after reperfusion. Scenarios involving less severe ischemia or varying durations of reperfusion were not assessed as the full spectrum of clinical presentations of ACSs is inherently impossible to model in this proof of concept study. As the time course of selectin expression following inflammatory insult has been well characterized in other studies, extrapolation of these studies would predict persistent E-selectin expression for up to 24 hours.[34] Regarding the relevance of our method to lesser degrees of ischemia, partial or briefer coronary occlusion of any clinical significance is likely to cause an inflammatory response associated with leukocyte adhesion molecule upregulation. Thus, a diagnostic imaging approach targeting leukocyte adhesion molecules should detect clinically relevant or significant ischemic events. Future studies with imaging at earlier or later time points after reperfusion will help further define the time window during which this technique has greatest sensitivity and specificity.

We did not measure serum troponin levels to compare the sensitivity of UMI to standard clinical biomarkers. However, our histochemical stain (TTC) detected no infarction, from which we infer that serum troponin levels would have been negligible in our experiments.

We used open-chest imaging, although closed-chest imaging, such as would be employed in the clinical setting, may be less sensitive for detection of adhered MBs. As we were seeking proof of concept, we strove to optimize image quality, and the narrow intercostal spaces in rats precluded satisfactory placement of the imaging transducer to generate high-quality images. We would anticipate this to be a less severe constraint in human application.

Toxicology studies were not performed. The biotinstreptavidin interaction to attach the peptide to the MB shell is potentially immunogenic. In future translation of this

methodology, alternatives such as maleimide linkage of the peptide or polyethylene glycol–based linkages to the MB can be used. Potential immunogenicity and toxicity of the peptide-covered MB could exist, even though no obvious toxicity was encountered during the acute use of the construct. The peptides used in this study were 12-mers, and the total peptide housed by the MBs was in the nanogram range.

Conclusions

We developed an approach to the ultrasonic diagnosis of recent myocardial ischemia using polymer MBs conjugated with E-selectin-specific peptide. A nonligand conjugated formulation of the MB contrast agent used in this study has been tested safely in humans in the past, which should facilitate the clinical translation of the targeted agent, offering a new modality for the diagnosis of ACSs in patients presenting to the emergency department with chest pain.

Acknowledgments

We thank Michele Grata, Linda Lavery, and Abigail Schwartz for their technical assistance and Dr. Tom Ottoboni for supplying the peptides and MBs and helpful discussions.

Financial disclosure of authors: This work was supported by the National Institutes of Health (R01HL077534 and RC1EB010533) and the Center for Ultrasound Molecular Imaging and Therapeutics at the University of Pittsburgh (F.S.V., J.W., X.C., A.C.). Dr. Leng was supported by the Natural Science Foundation of China (no. 30900367, 81371569).

References

1. Krieglstein CF, Granger DN. Adhesion molecules and their role in vascular disease. Am J Hypertens. 2001; 14:44S–54S. doi:10.1016/ S0895-7061(01)02069-6. [PubMed: 11411765]
2. Nakamori S, Kameyama M, Imaoka S, et al. Involvement of carbohydrate antigen sialyl Lewisx in colorectal cancer metastasis. Dis Colon Rectum. 1997; 40:420–31. doi:10.1007/BF02258386. [PubMed: 9106690]
3. Villanueva FS, Lu E, Bowry S, et al. Myocardial ischemic memory imaging with molecular echocardiography. Circulation. 2007; 115:345–52. doi:10.1161/CIRCULATIONAHA.106.633917. [PubMed: 17210843]
4. Cao H, Huang S, Cheng J, et al. Chemical preparation of sialyl Lewis x using an enzymatically synthesized sialoside building block. Carbohydr Res. 2008; 343:2863–9. doi:10.1016/j.carres.2008.06.020. [PubMed: 18639240]
5. Ravindranath NM, Nishimoto K, Chu K, Shuler C. Cell-surface expression of complement restriction factors and sialyl Lewis antigens in oral carcinoma: relevance to chemo-immunotherapy. Anticancer Res. 2000; 20:21–6. [PubMed: 10769630]
6. Ogiso M, Shogomori H, Hoshi M. Localization of LewisX, sialyl-LewisX and alpha-galactosyl epitopes on glycosphingolipids in lens tissues. Glycobiology. 1998; 8:95–105. doi:10.1093/glycob/8.1.95. [PubMed: 9451018]
7. Wei K, Crouse L, Weiss J, et al. Comparison of usefulness of dipyridamole stress myocardial contrast echocardiography to technetium-99m sestamibi single-photon emission computed tomography for detection of coronary artery disease (PB127 multicenter phase 2 trial results). Am J Cardiol. 2003; 91:1293–8. doi:10.1016/S0002-9149(03)00316-3. [PubMed: 12767419]
8. Main ML, Ehlgen A, Coggins TR, et al. Pulmonary hemodynamic effects of dipyridamole infusion in patients with normal and elevated pulmonary artery systolic pressure receiving PB127. J Am Soc Echocardiogr. 2006; 19:1038–44. doi:10.1016/j.echo.2006.03.006. [PubMed: 16880100]

9. Villanueva FS, Gertz EW, Csikari M, et al. Detection of coronary artery stenosis with power Doppler imaging. Circulation. 2001; 103:2624–30. doi:10.1161/01.CIR.103.21.2624. [PubMed: 11382734]
10. Ottoboni S, Short RE, Kerby MB, et al. Characterization of the in vitro adherence behavior of ultrasound responsive double-shelled microspheres targeted to cellular adhesion molecules. Contrast Media Mol Imaging. 2006; 1:279–90. doi:10.1002/cmmi.115. [PubMed: 17191768]
11. Martens CL, Cwirla SE, Lee RY, et al. Peptides which bind to E-selectin and block neutrophil adhesion. J Biol Chem. 1995; 270:21129–36. doi:10.1074/jbc.270.36.21129. [PubMed: 7545665]
12. Villanueva FS, Jankowski RJ, Manaugh C, Wagner WR. Albumin microbubble adherence to human coronary endothelium: implications for assessment of endothelial function using myocardial contrast echocardiography. J Am Coll Cardiol. 1997; 30:689–93. doi:10.1016/S0735-1097(97)00197-6. [PubMed: 9283527]
13. Lindner JR, Song J, Xu F, et al. Noninvasive ultrasound imaging of inflammation using microbubbles targeted to activated leukocytes. Circulation. 2000; 102:2745–50. doi:10.1161/01.CIR.102.22.2745. [PubMed: 11094042]
14. Weller GE, Lu E, Csikari MM, et al. Ultrasound imaging of acute cardiac transplant rejection with microbubbles targeted to intercellular adhesion molecule-1. Circulation. 2003; 108:218–24. doi:10.1161/01.CIR.0000080287.74762.60. [PubMed: 12835214]
15. Fishbein MC, Meerbaum S, Rit J, et al. Early phase acute myocardial infarct size quantification: validation of the triphenyl tetrazolium chloride tissue enzyme staining technique. Am Heart J. 1981; 101:593–600. doi:10.1016/0002-8703(81)90226-X. [PubMed: 6164281]
16. Kaufmann BA, Lewis C, Xie A, et al. Detection of recent myocardial ischaemia by molecular imaging of P-selectin with targeted contrast echocardiography. Eur Heart J. 2007; 28:2011–7. doi:10.1093/eurheartj/ehm176. [PubMed: 17526905]
17. Porter TR. Cardiovascular imaging of remote myocardial ischemia: detecting a molecular trace of evidence left behind. Circulation. 2007; 115:292–3. doi:10.1161/CIRCULATIONAHA.106.675413. [PubMed: 17242293]
18. Klibanov AL, Rychak JJ, Yang WC, et al. Targeted ultrasound contrast agent for molecular imaging of inflammation in high-shear flow. Contrast Media Mol Imaging. 2006; 1:259–66. doi:10. 1002/cmmi.113. [PubMed: 17191766]
19. Burt CW. Summary statistics for acute cardiac ischemia and chest pain visits to United States EDs, 1995-1996. Am J Emerg Med. 1999; 17:552–9. doi:10.1016/S0735-6757(99)90195-X. [PubMed: 10530533]
20. Brieger D, Eagle KA, Goodman SG, et al. Acute coronary syndromes without chest pain, an underdiagnosed and undertreated high-risk group: insights from the Global Registry of Acute Coronary Events Chest. 2004; 126:461–9. doi:10.1378/chest.126.2.461.
21. Christenson J, Innes G, McKnight D, et al. Safety and efficiency of emergency department assessment of chest discomfort. CMAJ. 2004; 170:1803–7. doi:10.1503/cmaj.1031315. [PubMed: 15184334]
22. Achar SA, Kundu S, Norcross WA. Diagnosis of acute coronary syndrome. Am Fam Physician. 2005; 72:119–26. [PubMed: 16035692]
23. Tucker JF, Collins RA, Anderson AJ, et al. Early diagnostic efficiency of cardiac troponin I and troponin T for acute myocardial infarction. Acad Emerg Med. 1997; 4:13–21. doi:10. 1111/j.1553-2712.1997.tb03637.x. [PubMed: 9110006]
24. Bremerich J, Buser P, Bongartz G, et al. Noninvasive stress testing of myocardial ischemia: comparison of GRE-MRI perfusion and wall motion analysis to 99 mTc-MIBI-SPECT, relation to coronary angiography. Eur Radiol. 1997; 7:990–5. doi:10.1007/s003300050238. [PubMed: 9265660]
25. Oudkerk M, Stillman AE, Halliburton SS, et al. Coronary artery calcium screening: current status and recommendations from the European Society of Cardiac Radiology and North American Society for Cardiovascular Imaging. Eur Radiol. 2008; 18:2785–807. doi:10.1007/s00330-008-1095-6. [PubMed: 18651153]

26. Ruiz M, Takehana K, Petruzella FD, et al. Arbutamine stress perfusion imaging in dogs with critical coronary artery stenoses: (99m)Tc-sestamibi versus (201)Tl. J Nucl Med. 2002; 43:664–70. [PubMed: 11994532]
27. Vanhaecke J, Flameng W, Borgers M, et al. Evidence for decreased coronary flow reserve in viable postischemic myocardium. Circ Res. 1990; 67:1201–10. doi:10.1161/01.RES.67.5.1201. [PubMed: 2225354]
28. Villanueva FS, Glasheen WP, Sklenar J, Kaul S. Characterization of spatial patterns of flow within the reperfused myocardium by myocardial contrast echocardiography. Implications in determining extent of myocardial salvage. Circulation. 1993; 88:2596–606. doi:10.1161/01.CIR.88.6.2596. [PubMed: 8252670]
29. Dilsizian V, Bateman TM, Bergmann SR, et al. Metabolic imaging with beta-methyl-p-[(123)I]-iodophenyl-pentadecanoic acid identifies ischemic memory after demand ischemia. Circulation. 2005; 112:2169–74. doi:10.1161/CIRCULATIONAHA.104.530428. [PubMed: 16186423]
30. Walzog B, Gaehtgens P. Adhesion molecules: the path to a new understanding of acute inflammation. News Physiol Sci. 2000; 15:107–13. [PubMed: 11390891]
31. Scholz D, Devaux B, Hirche A, et al. Expression of adhesion molecules is specific and time-dependent in cytokine-stimulated endothelial cells in culture. Cell Tissue Res. 1996; 284:415–23. doi:10.1007/s004410050602. [PubMed: 8646761]
32. Weyrich AS, Buerke M, Albertine KH, Lefer AM. Time course of coronary vascular endothelial adhesion molecule expression during reperfusion of the ischemic feline myocardium. J Leukoc Biol. 1995; 57:45–55. [PubMed: 7530283]
33. Davidson BP, Kaufmann BA, Belcik JT, et al. Detection of antecedent myocardial ischemia with multiselectin molecular imaging. J Am Coll Cardiol. 2012; 60:1690–7. doi:10.1016/j.jacc.2012.07.027. [PubMed: 23021335]
34. Fries JW, Williams AJ, Atkins RC, et al. Expression of VCAM-1 and E-selectin in an in vivo model of endothelial activation. Am J Pathol. 1993; 143:725–37. [PubMed: 7689792]

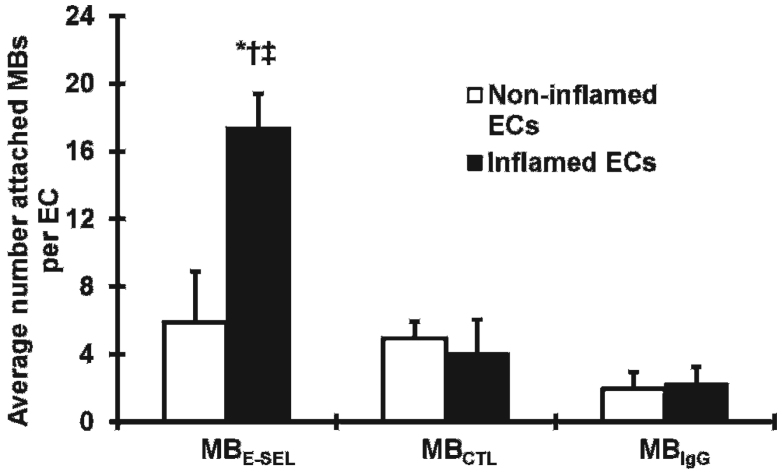

Figure 1.

Microbubble adhesion to rat microvascular endothelial cells (ECs) in vitro. *$p < .02$ for MB_{ESEL} in inflamed ECs versus noninflamed ECs. †$p < .02$ for MB_{ESEL} versus MB_{CTL} in inflamed ECs. ‡$p < .01$ for MB_{ESEL} versus MB_{IgG} in inflamed ECs.

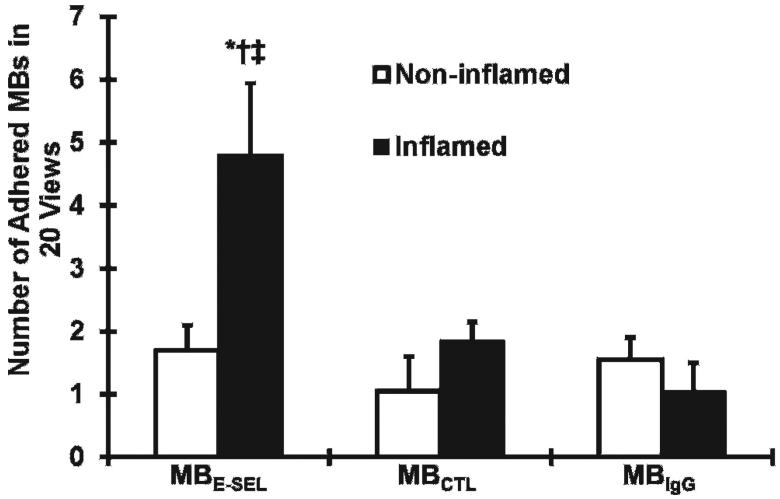

Figure 2.

In vivo adherence of E-selectin targeted and control micro-bubbles (MBs) to rat cremaster microcirculation. *$p < .04$ MB_{ESEL} in inflamed versus noninflamed microcirculation. †$p < .04$ MB_{ESEL} versus MB_{CTL} in inflamed microcirculation. ‡$p = .03$ MB_{ESEL} versus MB_{IgG} in inflamed microcirculation.

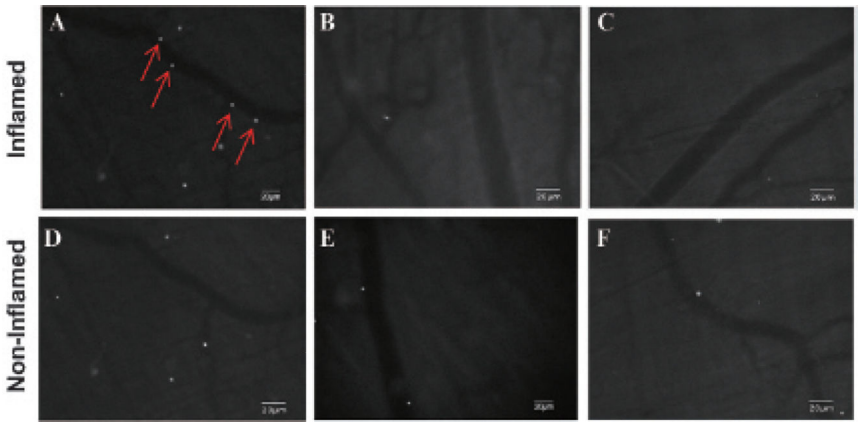

Figure 3.

Fluorescent micrographs of rat cremaster microcirculation. Fluorescent microbubble attachment under TNF-α-induced inflammation (A, B, C) or basal conditions (D, E, F) after intravenous MB_{ESEL} (A, D), MB_{CTL} (B, E), and MB_{IgG} (C, F). After MB_{ESEL} injection, there was adhesion to inflamed circulation (*arrows*) but not to control, nonin-flamed circulation. There was minimal adhesion of the control microbubbles to normal or inflamed circulation.

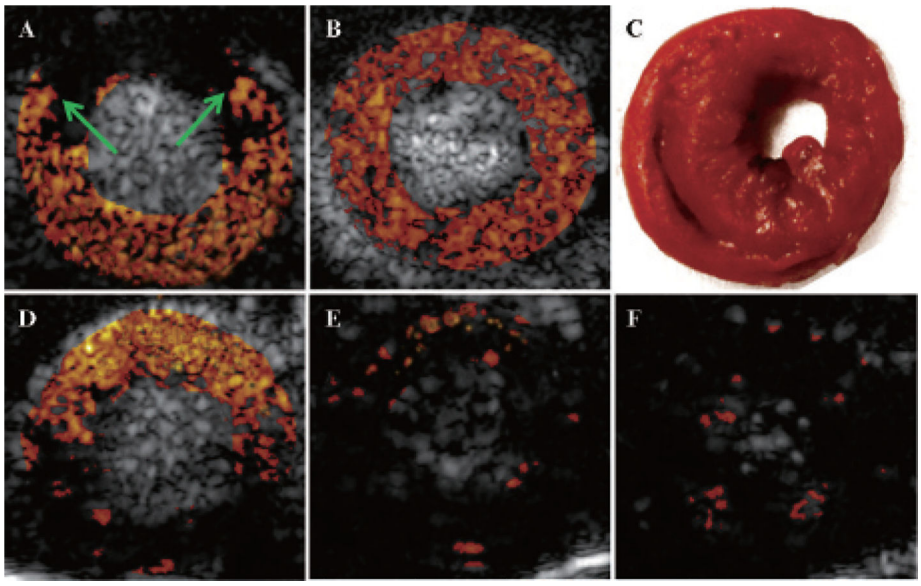

Figure 4.

Background-subtracted, color-coded ultrasound contrast images of the left ventricle in the short-axis view during coronary occlusion (A) and 4 hours after reperfusion (B, D to F). *A*, During coronary occlusion and injection of nontargeted microbubbles, there was a risk area (region between the *arrows*), corresponding to the left anterior descending (LAD) coronary artery territory. *B*, During reperfusion and injection of nontargeted micro-bubbles, there was homogeneous contrast enhancement of the myocardium. *C*, There was no infarction by triphenyl tetrazolium chloride staining. *D*, After injection of MB_{ESEL}, there was persistent contrast enhancement of the previously ischemic LAD coronary artery territory, not seen after injection of either of the MB_{CTL} (E) or MB_{IgG} (F).

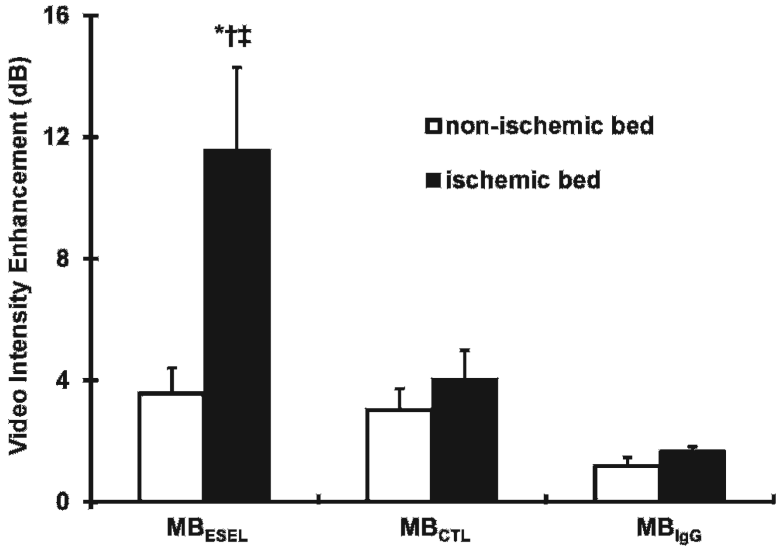

Figure 5.

Videointensity measurements in the postischemic and nonischemic regions after injection of three microbubble types. *$p < .02$ MB_{ESEL} in ischemic bed versus nonischemic bed. †$p < .03$ MB_{ESEL} versus MB_{CTL} in ischemic bed. ‡$p = .03$ MB_{ESEL} versus MB_{IgG} in ischemic bed.

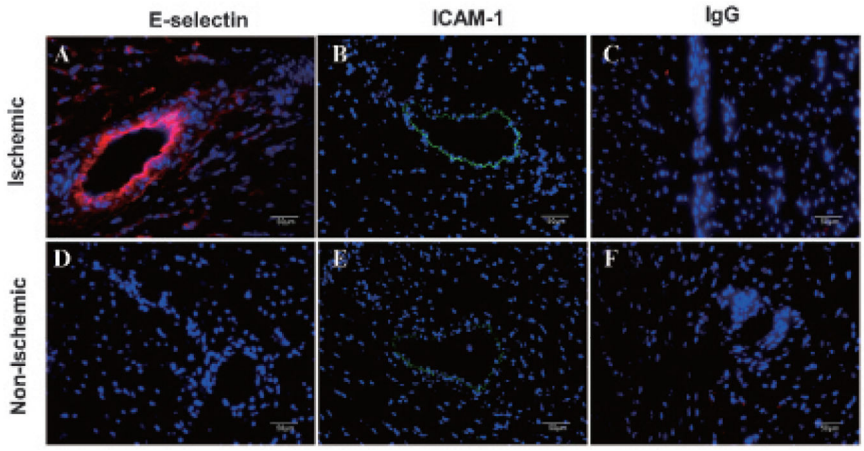

Figure 6.

Immunofluorescent staining of postischemic (A–C) and nonischemic (D–F) myocardium 4 hours afterreperfusion.Nucleiwerestainedblue with 4’,6-diamidino-2-phenylindole, E-selectin was stained red with CY3, and ICAM-1 was stained green with FITC. Nonspecific IgG was a control stain.